The optical design for the Giant Magellan Telescope Multi-object Astronomical and Cosmological Spectrograph (GMACS)

Ribeiro, Rafael A.S., Schmidt, Luke, Jones, Damien, Taylor, Keith, Prochaska, Travis, et al.

Rafael A.S. Ribeiro, Luke M. Schmidt, Damien Jones, Keith Taylor, Travis Prochaska, Erika Cook, Darren L. DePoy, Daniel Faes, Cynthia Froning, Tae-Geun Ji, Hye-In Lee, Jennifer L. Marshall, Claudia Mendes de Oliveira, Soojong Pak, Casey Papovich, Aline Souza, "The optical design for the Giant Magellan Telescope Multi-object Astronomical and Cosmological Spectrograph (GMACS)," Proc. SPIE 10702, Ground-based and Airborne Instrumentation for Astronomy VII, 107029B (12 July 2018); doi: 10.1117/12.2312814

SPIE.

Event: SPIE Astronomical Telescopes + Instrumentation, 2018, Austin, Texas, United States

The optical design for the Giant Magellan Telescope Multi-object Astronomical and Cosmological Spectrograph (GMACS)

Rafael A. S. Ribeiro*[a], Luke M. Schmidt[b], Damien Jones[c], Keith Taylor[d], Travis Prochaska[b], Erica Cook[b], Darren L. DePoy[b], Daniel Faes[a], Cynthia Froning[b], Tae-Geun Ji[e], Hye-In Lee[e], Jennifer L. Marshall[b], Claudia Mendes de Oliveira[a], Soojong Pak[e], Casey Papovich[b], Aline Souza[a]

[a]Department of Astronomy, IAG, Universidade de São Paulo (USP), São Paulo, Brazil
[b]Department of Physics and Astronomy, Texas A&M University, 4242 TAMU, College Station, TX, 77843-4242 USA
[c]Prime Optics, Australia; Department of Astronomy, C1400
[d]Instruments4, CA 91011, USA
[e]Kyung Hee University, Republic of Korea

ABSTRACT

We describe the optical design of GMACS, a multi-object wide field optical spectrograph currently being developed for the Giant Magellan Telescope (GMT). Optical spectrographs for the emerging generation of Extreme Large Telescopes (ELTs) have unique design issues. For example, the combination of both the largest field of view practical and beam widths achieving the desired spectral resolutions force the design of seeing limited ELT optical spectrographs to include large refractive elements, which in turn requires a compromise between the optical performance, manufacturability, and operability. We outline the details of the GMACS optical design subsystems, their individual and combined optical performance, and the preliminary flexure tolerances. Updates to the detector specifications, field acquisition/alignment optics, and optical considerations for active flexure control are also discussed. The resulting design meets the technical instrument requirements generated from the GMACS science requirements, is expected to satisfy the available project budget, and has an acceptable level of risk for the subsystem manufacture and assembly.

Keywords: Giant Magellan Telescope, Extremely Large Telescopes, Spectrograph, GMACS, Multi-object

1. INTRODUCTION

The Giant Magellan Telescope Multi-object Astronomical and Cosmological Spectrograph (GMACS) is a first light instrument for the GMT. It will be capable of obtaining spectroscopy of ultra-faint targets that are currently identified only from broad-band imaging observations. High throughput, simultaneous wide wavelength coverage, accurate and precise sky subtraction, moderate resolution, multi-object capabilities, relatively wide field, and substantial multiplexing are crucial design drivers for the instrument. It is expected that GMACS will form one of the most important and heavily utilized scientific capabilities of the GMT.[1] It is currently being designed by a collaboration consisting of scientists and engineers from Texas A&M University and the University of Texas in the USA, the University of São Paulo in Brazil, Kyung Hee University in South Korea, and Arizona State University in USA.

GMACS current optical design consists of a double-beam optical spectrograph comprising a split collimator, a dichroic beam-splitter, a set of volume-phase holographic transmission gratings (VPHGs) as the disperser, a set of passband filters for waveband selection, feeding twin red and blue optimized CCD cameras. Previous concepts were presented by DePoy et al.,[1] Jacoby et al.,[2] Schmidt et al.[3] and Prochaska et al.[4]

*rafael.alves.ribeiro@usp.br, phone:+55-16-99724-8887; http://www.iag.usp.br/astronomia/

Ground-based and Airborne Instrumentation for Astronomy VII, edited by Christopher J. Evans, Luc Simard, Hideki Takami, Proc. of SPIE Vol. 10702, 107029B · © 2018 SPIE · CCC code: 0277-786X/18/$18 · doi: 10.1117/12.2312814

GMACS is currently in its conceptual design and will undergo a midpoint conceptual design review in July of 2018 with the full conceptual design review the following March.

Additional GMACS project information can be found also in this conference in the overview (10702-69), optomechanical (10702-364), electronics (10702-365) and system engineering (10705-46) papers.

This paper is structured as follow: Sec.2 outlines the requirements for the optical design development; Sec.3 describes the current GMACS subsystem optical design, the detector layout, the split collimator and the cameras, followed by the spectrograph performance in Sec.4. Sec.5 describes preliminary flexure sensitivity analysis and Sec.6 reports on the updates of the field acquisition, alignment, and focus monitoring optics.

2. GMACS REQUIREMENTS

Through collaboration with the Giant Magellan Telescope Organization (GMTO), its partners and other representatives from the scientific community, a set of principal functional requirements have been developed. A 2014 GMACS community workshop included more than 50 participants from GMT partner and non-partner institutions with broad scientific interests. The recommendations of this meeting were integrated into the GMACS scientific requirements and subsequently flowed down to the definition of the GMACS functional parameters, Tab.1.

Table 1: GMACS Principal Optical Functional Parameters.

Parameter	**Requirement**
Field of View	30-50 arcmin sq.
Wavelength Coverage	Blue cut-off: 320-350 nm*
	Red cut-off: 950-1000 nm
Spectral Resolution	Blue: 1000-6000
	Red 1000-6000
Image Quality	80% EE† at 0.15-0.30 arcsec diameter
Spectral Stability	0.1-0.3 spectral resolution elements/hour

* 320 nm is highly desirable
† EE: Encircled Energy. EE80 means 80% of encircled energy

The Field of View (FoV) requirement corresponds to a circle of approximately 6.2 and 8.0 arcmin diameter for the 30 and 50 arcmin square respectively. The wavelength coverage for high-resolution mode may be compromised, but full coverage is required at the lowest resolutions. The spectral stability is mainly affected by flexure due to gravity and temperature variations and whose predicted consequences represent a critical role in the trade-off analysis for the optical design architecture.

GMACS is designed for the Direct Gregorian Narrow-Field (DGNF) configuration of the GMT. The current GMACS optical system design does not include an atmospheric dispersion compensator or wide-field corrector. The Radius of Curvature (RoC) of the GMT focal plane is about 2.200mm concave towards the instrument.

GMACS will interface with MANIFEST, the GMT fiber positioner system, in order to have access to the full GMT uncorrected 20 arcmin diameter field of view. Therefore, GMACS must have sufficient optical performance to take advantage of the reduced slit width of the fiber output that will allow higher resolution observations with the combined GMACS-MANIFEST system. MANIFEST is also presented in this conference (10702-372).

3. OPTICAL DESIGN

The current GMACS optical system is based on a refractive split collimator architecture. The red and blue arms each contain a selectable Volume Phase Holographic Grating (VPHG), articulated camera with a shutter and optional filter, and a 12k x 8k pixel CCD mosaic. The collimator is $f/8.2$ with 2,200mm effective focal length (EFL) and 7.4 arcmin FoV, which images the GMT entrance pupil onto the grating planes while splitting the incoming light by a tilted dichroic into two spectral bands corresponding to the blue arm (320nm to 600nm)

and the red arm (500nm to 1000nm). The collimator exit pupil diameter is 270mm, which defines the minimum size of the VPHG. The dispersed beams are imaged by two independent articulated f/2.2, 594mm EFL cameras operating in transmission Littrow. The dichroic transition is set at 557.7 nm, a bright atmospheric emission line, and the steepness of the dichroic transition will determine the spectral overlap required to generate a complete spectrum.

The guidelines for development of the collimator and cameras are shown in Tab.2. All the GMACS optical elements comprise singlets, air-doublets or air-triplets to avoid the use of cemented or coupled optics.

Table 2: Guidelines for GMACS optical design

Feasibility requires:	Low UV-VIS material internal absorption; Availability of large optical glass blanks.
Higher throughput requires:	Minimize the number of air-glass interfaces; Only FS and CaF_2 materials for the blue arm lenses (both the blue arm split collimator and blue camera).
Material restriction consequences:	Difficult to get color corrections (Secondary and Transverse Chromatic Aberration); Increase the number of elements to achieve acceptable performance.
Avoiding cemented optics leads to:	Increase the number of air-glass interfaces; Increase the necessity for aspherical surfaces.
Vignetting effects:	Results in better performance for large fields; Reduce spectral flux as function of field and wavelength.

3.1 Detector

The detector focal planes are assumed to be a 2-by-3 mosaic of $4k^2$ with $15\mu m$ pixel pitch CCDs forming an effective sensor array of 12,288 x 8,192 pixels (dimension of 184.32mm x 122.88mm, considering 100% fill factor), Fig.1. The shorter dimension is assumed to be the "spatial direction" and the longer the "spectral direction".

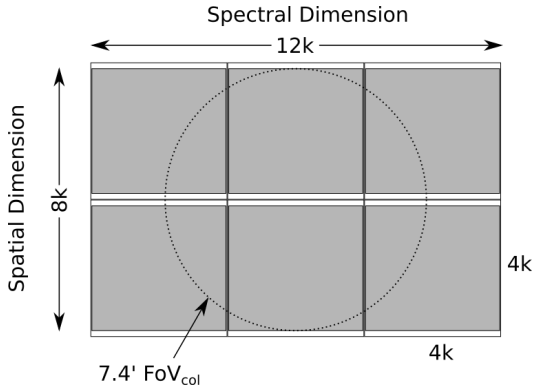

Figure 1: 12k-by-8k CCD mosaic forming the sensor assembly for the GMACS. The collimator FoV is shown by the dashed circle whose diameter is enclosed within the smaller sensor dimension. It is assumed that the dispersion direction is in the orthogonal dimension.

The objects imaged by GMACS are within the FoV of 7.4arcmin, which is limited by the collimator focal length and the maximum available grating diameters. The cameras FoV provide the remaining field to image the dispersed beam on the total area of the detector, along the spectral direction.

We are investigating the possibility of single-sided readout detectors to avoid the larger gap between the two sets of the horizontal 3x1 detectors required by the standard dual-sided readout CCDs shown in Fig.1.

3.2 Split Collimator

The layout of the split collimator is illustrated in Fig.2. It generates an image of the telescope entrance pupil, located at its primary multiple mirror system, in the vicinity of the VPHG. The pupil aberrations are tightly controlled due to strong astigmatism and field curvature so as not to overload the corrections needed by the cameras. The convex radius of curvature of the telescope focal plane is ≈2,200mm formed at f/8.16 giving an image diameter of ≈450 mm for a 7.4 arcminute field of view (FoV).

The positive spherical fused silica (FS) Field Lens (FL) is the only optical element shared by both collimator arms. A wedged dichroic splits the beams feeding the two collimator arms. For the blue collimating arm, a plane mirror is used to accommodate space constraints, followed by the blue collimating group, a reverse telephoto group. All the glass materials for the blue collimator arm are FS and CaF_2 due to their excellent throughput in UV-blue spectral range. The red arm, which is comprised by a wedge fused silica second plate, referred to as "compensator", and the telephoto collimator group of PBL6Y, CaF_2 and BSM51Y glasses, is fed by the transmissive beam of the wedge dichroic. Both collimator groups have one aspheric surface, with Best Fit Spherical Deviation (BFSD) less than $200\mu m$, located in the second surface of the element closest to the collimator exit pupil, CaF_2 and BSM51Y for blue and red collimator arm, respectively.

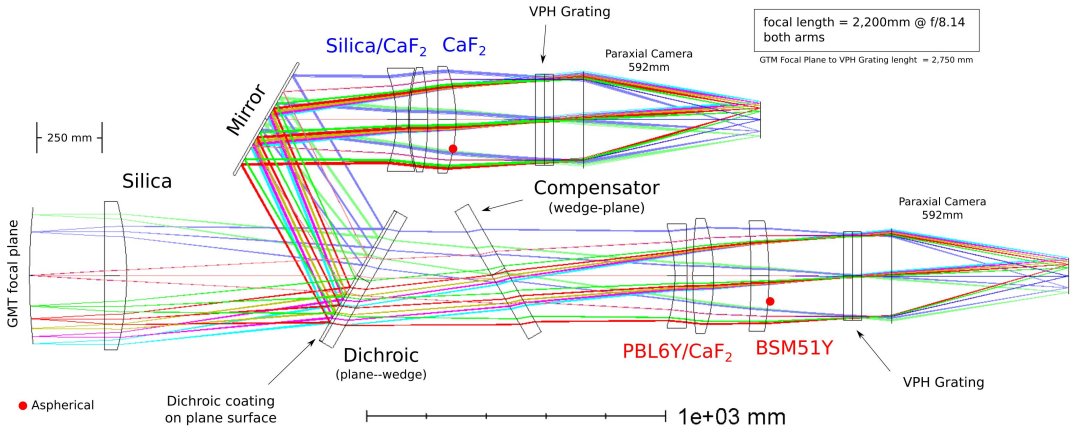

Figure 2: GMACS Split Collimator optical layout with paraxial cameras.

This design corrects astigmatism caused by the tilted dichroic by adding a second plate, referred to as "compensator", tilted in the opposite sense to the dichroic. Both the 2nd surface of the dichroic and the 1st surface of the compensator are given a small wedge, about 15 arcmin. Besides the fact that adding element impacts on the throughput, the resultant aberrations, including lateral color, are nearly entirely symmetric and thus intrinsically correctable. This solution will also eliminate the afore-mentioned manufacturability concerns from alternative solutions which use cylindrical surfaces and elements, Ribeiro et al.[5]

Both collimators have a pupil relief (the distance between the last collimator surface to the center plane of the VPHG) of about 270mm, to accommodate the grating rotation for the spectrograph high resolution mode.

The estimated throughput, excluding the GMT mirrors reflectance, the dichroic (either surfaces and internal material absorption) and considering a 99% transmittance of the AR coating, and 95% for mirror surface reflectance, is $T_{blue} \approx 82.3\%$ and $T_{red} \approx 86.0\%$, for the blue and red collimator arms, respectively.

Fig.3 shows the spot diagrams of the split collimator with a 594mm focal length paraxial camera for a circular FoV of 7.4 arcmin diameter. The reference circle is 0.3 arcsec in diameter. Not only the EE80 in 0.3 arcsec is met, but also all the geometric encircled energy falls within this circle. The transverse chromatic aberration, not shown, is less than $150\mu m$ for blue and $30\mu m$ for red for the full field.

The polarization effects caused by both the dichroic and the mirror in the blue collimator are yet to be examined.

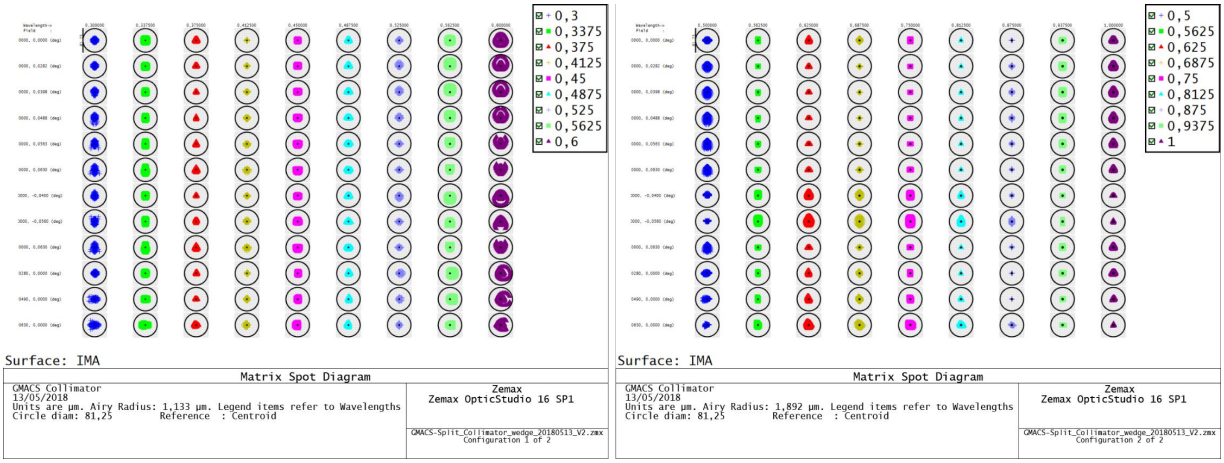

Figure 3: Spot diagram for the split collimator with 594mm focal length paraxial cameras. **Left**: blue arm from 300nm - 600nm. **Right**: red arm from 500nm to 1.000nm. The reference circle is 0.3 arcsec diameter.

3.3 Cameras

Both of the articulated GMACS cameras have identical optical parameters: f/2.2, 594mm EFL and the camera relief (the distance between the center plane of the VPHG to the first camera's surface) is about 270mm. The mechanisms for filter and shutter are close to the focal plane, a default 30mm thickness fused silica plate is used to simulate the filter.

Their optical performance is not shown because the last process for the optimization methodology for the GMACS optical system incorporates the GMT and the respective arm of the split collimator into the fine processes of each camera optimization. Therefore, the final cameras performances take into account the complete spectrograph system, described in Sec.4.

3.3.1 Blue Camera

The blue camera comprises eight elements of FS and CaF_2, Fig.4, because only these materials meet the requirements for high throughput (through their low internal absorbance in UV-Blue) and which large optical glass blanks are available (diameters of 1,500mm for FS and 400mm for CaF_2).

Two aspheric surfaces on positive CaF_2 lenses, marked with a red dot in Fig.4, help control the field aberrations. Their maximum deviation from best spherical fit are approximately $1,000\mu m$ and $240\mu m$, from the surfaces left to right of the Fig.4, with maximum slope of 5.4×10^{-2} and 1.2×10^{-2}, respectively.

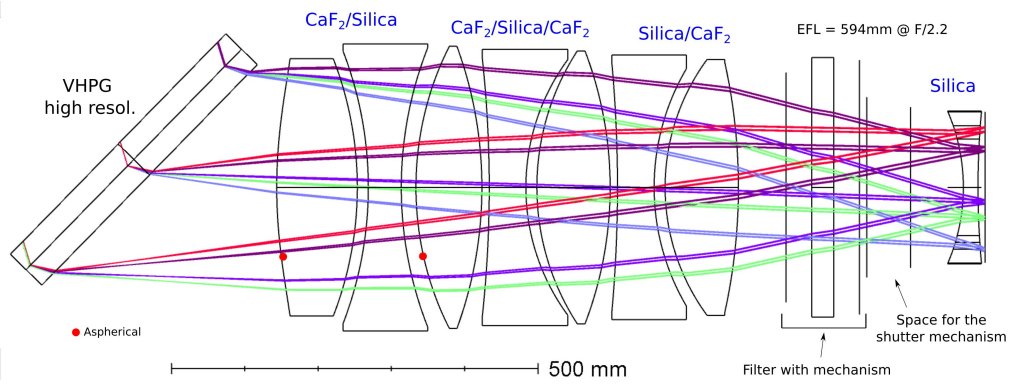

Figure 4: Blue camera optical layout.

The cameras have a field vignetting maximum of 5% at their extremities. This effect is considered negligible for low-resolution modes and acceptable for the high-resolution spectrograph modes because the field vignetting turns into spectral vignetting only for a small range at both extreme wavelengths and extreme fields.

The estimated blue camera throughput for the central field is $\approx 70\%$ throughout the blue spectral range, considering only the camera lenses, except the spectral filter (either surfaces and internal material absorption) and assuming a 99% transmittance of the AR coating of each surface. For large fields the throughput drops to $\approx 67\%$ due to the vignetted fields.

The design has acceptable axial color and spherochromatism aberrations, it presents $\approx 700\mu m$ of Transversal Chromatic Aberrations, TCA, which is ≈ 3.6 times the spectral resolution for a 0.7 arcsec slit. The consequences of the TCA in GMACS spectrograph modes are still under evaluation. If GMACS is used in image mode (no camera-collimator articulation), the large TCA forces the restriction of the camera spectral band through the use of an appropriate optical bandpass filter (about 30nm), resulting in a narrow bandwidth image.

3.3.2 Red Camera

The red camera comprises six lenses of FS, CaF_2, PBL6Y and BSM51Y, Fig.5. The larger availability of optical glass blanks for the red camera compared to the blue camera allows better overall aberration correction with fewer lenses, including TCA. A previous version of the red camera has two singlets (CaF_2 and FS) that replaces the aspherical CaF_2 singlet, Ribeiro et al.[5]

Two aspherical surface are located at the first and second positive CaF_2 lens with a spherical deviation approximately $350\mu m$ and $320\mu m$, and maximum slope of 1.4×10^{-2} and 1.5×10^{-2} (RMS of 6.3×10^{-3} and 5.6×10^{-2}), respectively. The estimated throughput is $\approx 73\%$ throughout the red spectral range, assuming a 99% transmittance of the AR coatings and the internal transmittance data from suppliers.

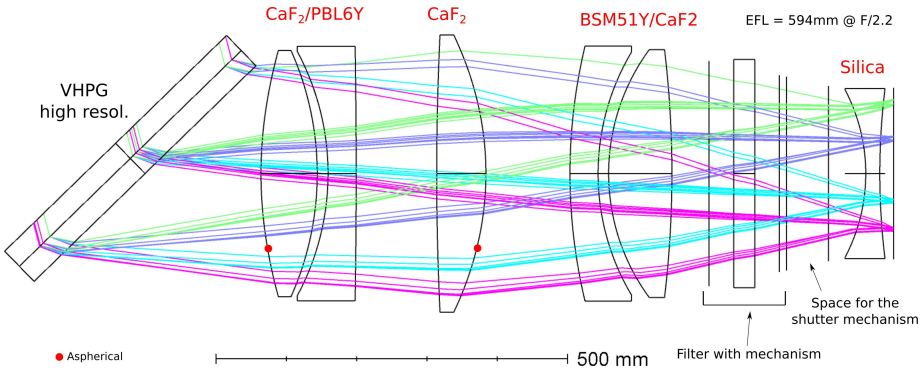

Figure 5: Red camera optical layout.

4. SPECTROGRAPH PERFORMANCE

The spectrograph performance described in this sections includes the GMT optical model and the GMACS blue and red arm independently.

4.1 Asymmetric fields

The GMACS optical system is asymmetric due to two factors: the grating intrinsic properties, and the combination of the dichroic and compensator of the split collimator. Therefore, for low-resolution mode, the field data are samples in several points within the 7.4 arcmin FoV diameter to account for any asymmetrical field behavior. For the high-resolution mode, the field data are sampled along a 7.4 arcmin long slit centered in the collimator FoV and parallel to the grating grooves, Fig.6.

(a) Field data for low resolution mode

(b) Field data for high resolution mode

Figure 6: Field data for both resolution modes, near to the GMT focal plane. The vertical axis is aligned to the grating lines. b) the fields are aligned to a center long slit

4.2 Blue Arm

The spot diagram for the GMACS blue arm is illustrated in Fig.7. The RMS EE80 is ≈ 0.1 arcsec and the RMS geometrical spot is ≈ 0.3 arcsec for all fields, wavelengths, and both resolution modes. The spots are referred to the centroid.

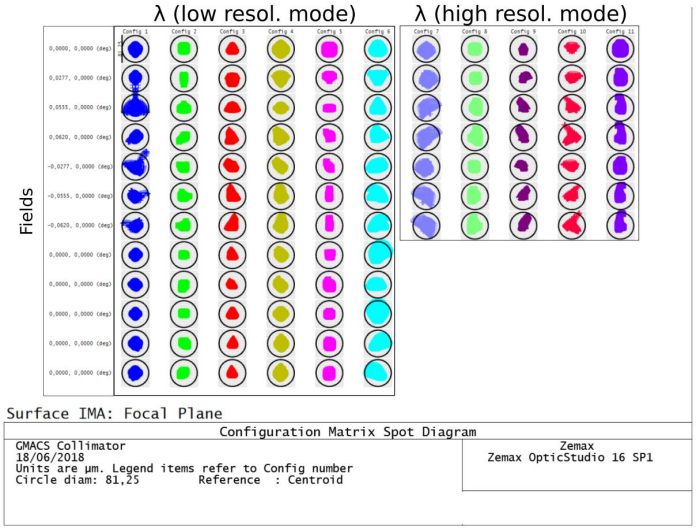

Figure 7: Blue arm spot diagram for both modes. The rows represent object fields and the columns represent the wavelength for the resolution mode highlighted on the top. The left highlighted rectangle is for low-resolution mode, from 320nm to 600nm, and the right for the high-resolution mode, from 460nm to 490nm (the central wavelength is selectable). The reference circle is 0.3 arcsec diameter.

The estimated throughput for GMACS blue arm, based on the considerations described in Tab.3, is $\approx 60\%$, and $\approx 56\%$ for the vignetted field and wavelengths. The TCA is $\approx 110\mu m$.

4.3 Red Arm

The spot diagram for the GMACS red arm is illustrated in Fig.8. The performance is similar to the blue arm: the RMS EE80 is ≈ 0.1 arcsec, and the RMS geometrical spot is ≈ 0.3 arcsec for all fields, wavelengths and both resolution modes. The spots are referred to the centroid.

The estimated throughput for the GMACS red arm is $\approx 62\%$, with the considerations given in Tab.3.

Table 3: Main considerations for throughput estimative

Both the GMT mirrors are 100% reflective
Fold mirror surface (split blue collimator) have 95% reflectance
All optical surfaces are AR coated with 99% transmittance (entire spectral range)
VPHG efficiency, dichroic, and filter performance are not considered (surface and internal material absorption)
Slit losses are not considered
Internal transmittance data from glass suppliers is considered

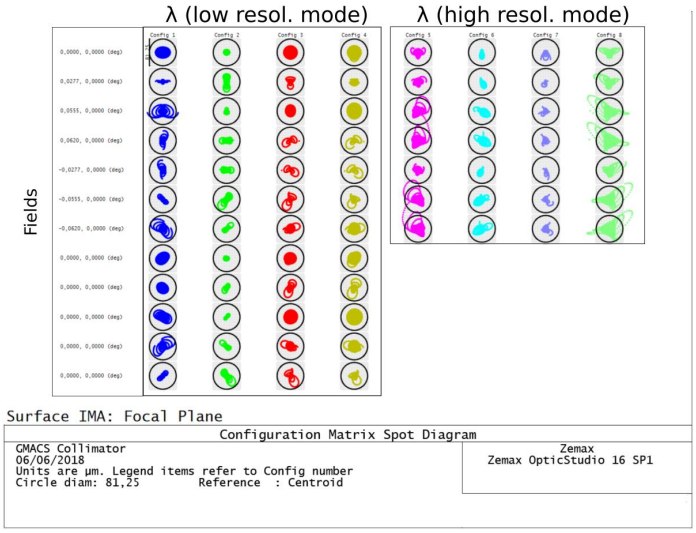

Figure 8: Red arm spot diagram. The left highlighted rectangle is for low-resolution mode, from 550nm to 950nm, and the right for the high-resolution mode, from 650nm to 750nm (the central wavelength is selectable). The reference circle is 0.3 arcsec diameter.

4.4 Resolution

GMACS is a flexible and configurable spectrograph which allows the users to have a broad range of resolution and bandwidth configurations within the GMACS spectral range of operation. The grating tilt mechanism, a selectable VPHG, the articulated cameras, and the possibility to change the slit width allow the selection of several spectrograph configurations. A few examples are demonstrated in Tab.4. The physical limitation is due to the maximum 90° tilt between the collimator and camera optical axis, i.e, blaze angle is chosen such that diffraction angle and incidence angle are identical and less than 45°.

5. TOLERANCE ANALYSIS

One of the main challenges related to the operability of the GMACS optical system is the spectral stability due to the flexure caused by the gravity vector. GMACS mounted at the Gregorian focus position of the GMT will experience a continually changing orientation as the telescope tracks an object across the sky during the integration time. Therefore, the gravity-induced flexure of the instrument must be monitored and compensated. A look-up table based compensation solution shall be difficult to address all the possible flexure due to the reconfigurable nature of GMACS . Thus the solution points towards an active compensator system.

Tab.1 shows that spectral stability required is equivalent to approximately $56.7\mu m$ at the focal plane (i.e., 3.8 pixels, considering the focal plane described in Sec.3.1), for a slit width of 0.7 arcsec. The goal reduces this

Table 4: Examples for spectrograph configurations

	Mode of operation	Slit width $[arcsec]$	θ_B* [°]	Grating groove $[lines/mm]$	λ_0† $[nm]$	Resol. at λ_0	$\Delta\lambda$‡ $[nm]$
Blue arm	Low resol.	0.7	5.0	410	435	720	250
	High resol.	0.7	32.0	2,800	370	3,800	95
		0.7	37.5	2,800	435	4,800	88
		0.7	44.4	2,800	500	6,100	80
	Mode of operation	**Slit width** $[arcsec]$	θ_B [°]	**Grating groove** $[lines/mm]$	λ_0 $[nm]$	**Resol. at** λ_0	$\Delta\lambda$ $[nm]$
Red arm	Low resol.	0.7	5.2	240	750	560	430
	High resol.	0.7	40.0	2,050	625	5.200	115
		0.7	44.2	2,050	680	6.000	100
		0.7	44.4	1,600	875	6.120	140

* Blazed angle for Littrow configuration to get the highest VPHG efficiency
† Center wavelength
‡ Spectral range

requirement to one third. A preliminary flexure sensitivity and inverse sensitivity analysis of the GMACS optical system is described in this section.

5.1 Preliminary Flexure Sensitivity Analysis

The primary objective of this study is to determine which of the groups and/or elements, as defined below, cause large spectral displacement in the focal plane due to tip and tilt perturbations. The secondary objective is to quantify which group is the best candidate to have active control, e.g., through a hexapod, to compensate for this flexure.

The only merit function applied to this analysis is the movement of the spot centroid on the focal plane due to the group/element decenter and tilt. This displacement is calculated as the vectorial composition of the spectral and spatial directions, as defined in Fig.1. This preliminary study does not consider EE80 variations due to these perturbations, possible spectral lines magnification or any effects which might degrade the image quality. A more realistic study will consider the Finite Element Analysis (FEA) results from flexure simulations of the GMACS structure due to the gravity vector influence.

Fig. 9 defines of the groups and elements for the GMACS blue arm. The dichroic is considered as a plane mirror, CG1. The blue collimator group, CG3 contains the reverse telephoto group of the blue split collimator arm. CG5 is the blue camera group and CG6 is the detector assembly group, comprised of the filter, shutter, and field flattener. Even though the field flattener is part of the camera, for clarity, CG5 is called the blue camera group. CG6 has a minimum of two degrees of freedom (DoF): one for focus adjustment (Z-axis) and spectral alignment in detectors arrays (about the Z-axis).

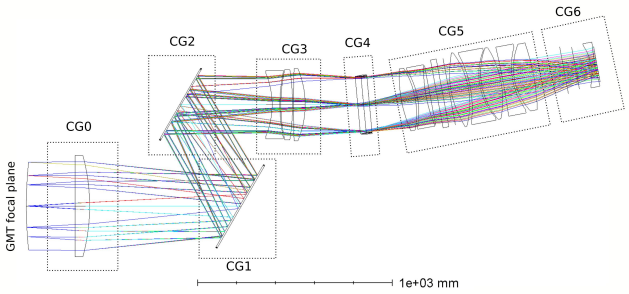

Group ID	Description
CG0	Field Lens
CG1	Dichroic (mirror)
CG2	Fold Mirror
CG3	Blue collimating group
CG4	VPHG
CG5	Blue camera group
CG6	Detector Group

Figure 9: Groups and elements definition for the GMACS blue arm.

The results are summarized in Tab.5. The axis origins (X, Y) are located locally for all the groups/elements. For large groups, CG3 and CG5, the origin is located in their geometrical centers, along with the Z-axis (optical axis). The correct interpretation of the table is as follow: a 1.5mm decenter of the CG0 (Field Lens) in X direction causes the spot centroid displacement of 0.3 times the spectral resolution element (which is $\approx 56.7\mu m$). The "Edge Displacement" is the distance the group/element moves at its border from the non-perturbed condition. Decenter and tilt are evaluated separately at this time (no combinations of decenter and tilt).

Table 5: Inverse Sensitivity analysis for the GMACS blue arm for 0.3 spectral resolution.

ID	**Description**	**Decenter (X,Y)** $[mm]$	**Tilt** $(\theta X, \theta Y)$ $[arcmin]$	**Edge Displacement** $(\theta X, \theta Y)$ $[\mu m]$**, eff. aperture**
CG0	Field Lens	1.4, 1.4	54.2, 54.2	3800, 3800 ($\phi \approx$ 480mm)
CG1	Dichroic (mirror)	n/a, n/a	0.44, 0.41	27, 25 ($\phi \approx$ 420mm)
CG2	Fold Mirror	n/a, n/a	0.28, 0.25	15, 13 ($\phi \approx$ 360mm)
CG3	Blue collimating group	0.25, 0.25	2.64, 2.64	123, 123 ($\phi \approx$ 320mm)
CG4	VPHG	n/a, n/a	60, 90	2800, 4200 ($\phi \approx$ 320mm)
CG5	Blue camera group	0.054, 0.054	2.7, 2.7	230, 220 ($\phi \approx$ 480mm)
CG6	Detector Group*	-	-	-

* Detector Group CG6 might be the focus (Z-axis) and roll compensator

Fig.10 defines the groups and elements for the GMACS red arm. Similar to the blue arm, the collimator red group, CG3 is comprised by the reverse telephoto group or the red split collimator arm. CG5 is the red camera group and CG6 is the detector assembly group, comprised by the filter, shutter, and field flattener.

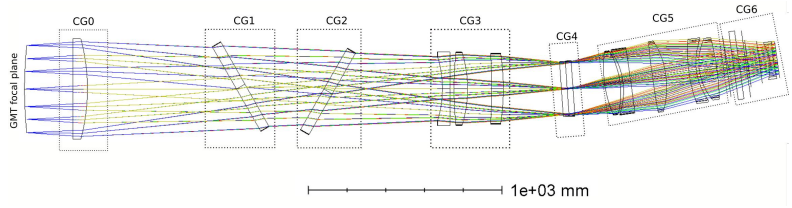

Group ID	Description
CG0	Field Lens
CG1	Dichroic
CG2	Compensator
CG3	Red collimating group
CG4	VPHG
CG5	Red camera group
CG6	Detector Group

Figure 10: Groups and elements definition for the GMACS red arm

The results are summarized in Tab.6 with the same interpretation as the previous table.

Table 6: Inverse Sensitivity analysis for the GMACS red arm for 0.3 spectral resolution shift

ID	Description	Decenter (X,Y) $[mm]$	Tilt (X,Y) $[arcmin]$	Tangential due Tilt (X,Y) $[\mu m]$, eff. aperture
CG0	Field Lens	1.5, 1.5	55.8, 55.8	3900, 3950 ($\phi \approx$ 480mm)
CG1	Dichroic	n/a, n/a	12, 12	840, 840 ($\phi \approx$ 480mm)
CG2	Compensator	n/a, n/a	7.8, 7.8	500, 500 ($\phi \approx$ 440mm)
CG3	Red collimating group	0.25, 0.25	2.1, 2.1	100, 100 ($\phi \approx$ 330mm)
CG4	VPHG	n/a, n/a	100, 100	4800, 4800 ($\phi \approx$ 320mm)
CG5	Red camera group	0.054, 0.054	5.5, 5.5	340, 340 ($\phi \approx$ 480mm)
CG6	Detector Group*	-	-	-

* Detector Group CG6 might be the focus (Z-axis) and roll compensator

5.2 Partial Conclusion

The dichroic-fold mirror combination is more than 20 times more sensitive to tilt in the blue arm compared to the red arm, as expected for a combination of mirrors in converging or diverging region of an imaging optical system. Both the collimator groups and camera groups sensitivities present similar performance, but the former is overall less sensitive than the latter. Therefore, the collimator groups might be good candidates for compensators in the GMACS flexure compensation system, as large decenter and tilt variations cause a small change in the spectral centroid position which allows for fine control of the spot positions. However, this partial conclusion does not preclude the possibility and even the necessity for including additional compensators in the camera and detector groups.

6. FIELD ACQUISITION AND ALIGNMENT OPTICS

The GMACS Guide, Acquisition, and Focus system (G-GAF) consists of multiple cameras placed at the edge of the GMACS spectroscopic field with a single movable camera that can be positioned behind the slit mask to confirm target object placement within a slit. This system determines the pointing offsets required for acquisition of target objects as well as maintaining their alignment with the slit mask throughout an observation. Both x-y motions and rotation of the mask relative to the sky are measured. The G-GAF also measures the location of the telescope focus relative to the GMACS slit mask and reports this value to the GMT AGWS system (Acquisition, Guiding, and Wavefront Control System) which will adjust any error in the telescope focus location due to any differential motion from flexure between the location of the AGWS and the slit mask.

Three fixed cameras, each with a field of view $\sim$1 arcmin in diameter will look through reference holes in the slit masks. Due to the large collecting area of the GMT, this field of view should be adequate to ensure that at least one appropriate guide star will be imaged at any pointing of the telescope.

In order to measure focus we are exploring a Hartmann prism concept shown in Figure 11. Each of the three $\sim f/4$ fixed cameras re-image the slit mask and would have the option to insert a Hartmann prism at the camera pupil. The central prism has no prism angle and generates the primary image. Light at the edges of the pupil pass through small angle prisms oriented 180° to each other. These produce fainter images on either side of the primary image. The images from prism one and three move in the opposite sense with a change in the telescope focus position relative to the slit mask. The focus offset and direction are quantified by measuring the slope of the line between images from prism one and three.

7. FUTURE WORK

GMACS is currently in its conceptual design which is scheduled to conclude in the first quarter of 2019.

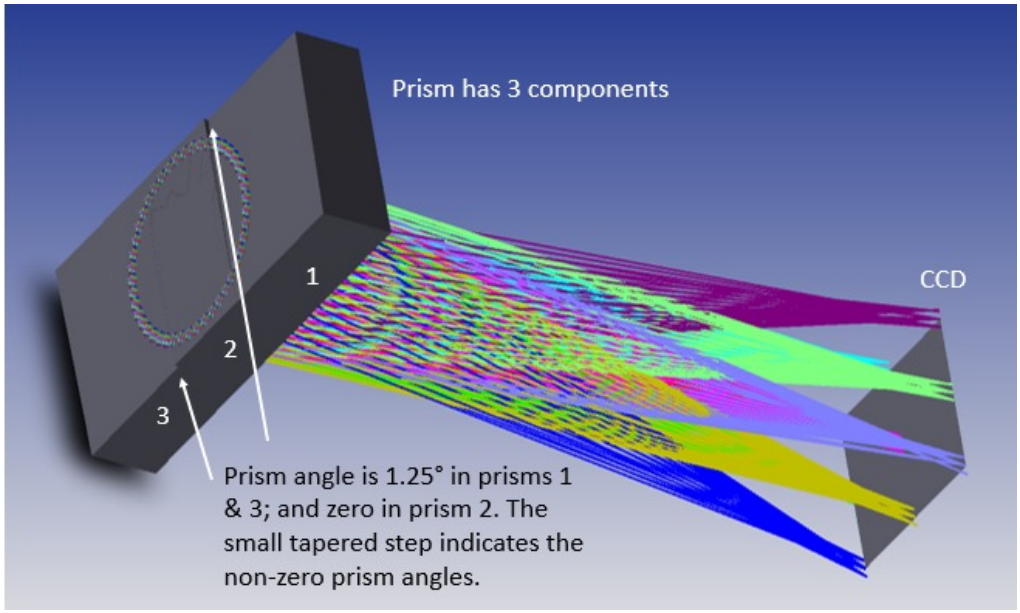

Figure 11: The G-GAF Hartmann prism concept for measuring the focus of the GMT relative to the GMACS slit mask.

The next design activities are related to the refinement of the optomechanical interfaces and incorporating feedback from optical vendors, the development of the guide camera optical design, and collaborating with the science team to determine the specifications for the first light gratings and filters. We will also maintain close cooperation with the MANIFEST optical team to ensure interoperability between the two instruments.

The subsequent tolerance analysis will incorporate FEA results of the gravity-induced flexure to define the performance requirements of the flexure compensation system and identify which optical groups are best suited for actuation to correct for flexure induced image motion. We will also investigate various optical metrology systems to provide feedback for the flexure compensation system.

High throughput, moderate resolutions, and broad wavelength coverage for many objects in a single observation both alone as well as in conjunction with MANIFEST will make GMACS a highly flexible first light instrument for the Giant Magellan Telescope, well suited to contribute to a wide variety of science topics.

ACKNOWLEDGMENTS

We are grateful for the financial support provided by GMT Brazilian Office and São Paulo Research Foundation (FAPESP), and Texas A&M University thanks Charles R. '62 and Judith G. Munnerlyn, George P. '40 and Cynthia Woods Mitchell, and their families for support of astronomical instrumentation activities in the Department of Physics and Astronomy.

REFERENCES

1. D. L. DePoy, R. Allen, R. Barkhouser, E. Boster, D. Carona, A. Harding, R. Hammond, J. L. Marshall, J. Orndorff, C. Papovich, K. Prochaska, T. Prochaska, J. P. Rheault, S. Smee, S. Shectman, and S. Villanueva, "GMACS: a wide field, multi-object, moderate-resolution, optical spectrograph for the Giant Magellan Telescope," *Proc. SPIE* **8446**, 2012.
2. G. H. Jacoby, R. Bernstein, A. Bouchez, M. Colless, J. Crane, D. DePoy, B. Espeland, T. Hare, D. Jaffe, J. Lawrence, J. Marshall, P. McGregor, S. Shectman, R. Sharp, A. Szentgyorgyi, A. Uomoto, and B. Walls, "Instrumentation progress at the Giant Magellan Telescope project," *Proc. SPIE* **9908**, 2016.

3. L. M. Schmidt, R. A. S. Ribeiro, K. Taylor, D. Jones, T. Prochaska, D. L. DePoy, J. L. Marshall, E. Cook, C. Froning, T.-G. Ji, H.-I. Lee, C. M. de Oliveira, S. Pak, and C. Papovich, "Optical design concept for the Giant Magellan Telescope Multi-object Astronomical and Cosmological Spectrograph (GMACS)," *Proc. SPIE* **9908**, 2016.
4. T. Prochaska, M. Sauseda, J. Beck, L. Schmidt, E. Cook, D. L. DePoy, J. L. Marshall, R. Ribeiro, K. Taylor, D. Jones, C. Froning, S. Pak, C. M. de Oliveira, C. Papovich, T.-G. Ji, and H.-I. Lee, "Optomechanical design concept for the Giant Magellan Telescope Multi-object Astronomical and Cosmological Spectrograph (GMACS," *Proc. SPIE* **9908**, 2016.
5. R. A. S. Ribeiro, L. M. Schmidt, , D. Jones, K. Taylor, T. Prochaska, D. L. DePoy, J. L. Marshall, E. Cook, C. Froning, T.-G. Ji, H.-I. Lee, C. M. de Oliveira, S. Pak, and C. Papovich, "Optical design concept for the Giant Magellan Telescope Multi-object Astronomical and Cosmological Spectrograph (GMACS): design methodology, issues, and trade-offs," *Proc. SPIE* **10690**, 2018.